

## Electrochemical characteristics of $\text{MnO}_2\text{-V}_2\text{O}_5$ composites serving as positive material for secondary lithium batteries\*

N. Kumagai, S. Tanifuji and K. Tanno

Dept. of Applied Chemistry, Faculty of Engineering, Iwate University, Ueda, Morioka 020 (Japan)

(Received January 2, 1991)

### Abstract

$\text{MnO}_2\text{-V}_2\text{O}_5$  composites formed by heating mixtures of  $\text{MnO}_2$  and  $\text{NH}_4\text{VO}_3$  under various conditions are evaluated as positive material for secondary lithium batteries. The charge/discharge characteristics of the composites are dependent on the type of  $\text{MnO}_2$  used, the heat-treatment temperature, the discharge rate, and the depth-of-discharge. A composite formed by heating a mixture of EMD and  $\text{NH}_4\text{VO}_3$  (V/Mn atom ratio=1.0) at 350 °C for 4 h in air exhibits the best cycling characteristics, and gives a discharge capacity of 250-350 A h/kg-oxide over 10 cycles at a current density of 0.20 mA cm<sup>-2</sup> at 25 °C in 1 M  $\text{LiClO}_4$ -propylene carbonate. X-ray diffraction, X-ray photoelectron spectroscopic, and SEM studies of the composite reveal that the charge/discharge characteristics may be determined by the structure of a surface layer formed on the  $\text{MnO}_2$  particles.

### Introduction

Much interest has centred in recent years on the development of secondary lithium batteries with high energy densities. Manganese dioxide has been widely used as a cathode material in lithium primary cells. Dampier [1] and Pistoia [2] have shown that  $\text{MnO}_2$  exhibits poor rechargeability in non-aqueous electrolytes. Recently, however, Nohma *et al.* [3] found that a lithiated material of the general formula,  $\text{Li}_x\text{MnO}_2$  ( $x$  being preferably 0.3-0.5), yields encouraging reversible behaviour.

This paper reports investigations of the electrochemical characteristics of  $\text{MnO}_2\text{-V}_2\text{O}_5$  composites when serving as a positive material for secondary lithium batteries.

### Experimental

The following  $\text{MnO}_2$  samples were used: (i) EMD, IBA (International Battery Materials Association Inc.) No. 17; (ii) CMD, IBA No. 22; (iii) NMD,

\*Paper presented at the 5th International Meeting on Lithium Batteries, Beijing, China, May 28-June 2, 1990.

IC (International Common) No. 7.  $\text{MnO}_2$ - $\text{V}_2\text{O}_5$  composites were prepared by heating mixtures of  $\text{MnO}_2$  and  $\text{NH}_4\text{VO}_3$  at a given V/Mn atomic ratio, and at various temperatures, for specific times in air. The  $\text{NH}_4\text{VO}_3$  was guaranteed reagent grade material supplied by the Kanto Chemical Co. Preparation of the electrodes and the electrochemical measurement techniques have been described previously [4]. The oxide composites were combined with graphite at a weight ratio of 1:1 and the resulting mixture was compression-moulded onto nickel mesh. The weight of the positive material was  $\sim 20 \text{ mg cm}^{-2}$ . Lithium pellets were used for both the negative and the reference electrodes. The discharge and recharge characteristics of the oxide electrodes were measured at several current densities, at  $25^\circ\text{C}$ , in a 1 M  $\text{LiClO}_4$ -propylene carbonate (PC) solution.

X-ray diffraction (XRD) measurements were performed using a Rigaku Denki Guinergflex 20B diffractometer with  $\text{Cu K}\alpha$  radiation. X-ray photoelectron spectroscopic (ESCA) data were obtained using a Dupont 650B spectrometer with  $\text{Mg K}\alpha$  radiation. The binding energy was calibrated with reference to the  $\text{C}_{1s}$  level of carbon (285.0 eV).

## Results and discussion

### *Heat-treated $\text{MnO}_2$ and $\text{NH}_4\text{VO}_3$ mixtures*

The XRD patterns of the products obtained from heating mixtures of  $\text{MnO}_2$  (EMD) and  $\text{NH}_4\text{VO}_3$  with a V/Mn atomic ratio of 1.0 and at different temperatures are shown in Fig. 1. It can be seen that the products obtained in the temperature range  $350$ – $500^\circ\text{C}$  consisted mainly of  $\text{V}_2\text{O}_5$  and  $\text{MnO}_2$ .  $\gamma/\beta$ - $\text{MnO}_2$  is present in the product formed at  $350^\circ\text{C}$ , but in the temperature range  $450$ – $500^\circ\text{C}$  it is converted to  $\beta$ - $\text{MnO}_2$  [2, 5]. Some new diffraction peaks ( $\square$  in Fig. 1) appear in the angular range  $27$ – $30^\circ 2\theta$ . The intensities of the peaks are very weak at  $350^\circ\text{C}$ , but they increase with rise in temperature at which the material is formed. These peaks may be due to the formation of a new surface phase on the  $\text{MnO}_2$  particles (see results of ESCA analysis discussed below). Finally, a double oxide,  $\text{Mn}_2\text{V}_2\text{O}_7$  was formed at  $700^\circ\text{C}$ , together with a small amount of  $\text{Mn}_2\text{O}_3$ .

The  $\text{Mn}_{2p}$ ,  $\text{V}_{2p}$  and  $\text{O}_{1s}$  ESCA spectra of the products formed between EMD and  $\text{NH}_4\text{VO}_3$  indicated that the products consist mainly of  $(\text{Mn}^{4+})(\text{O}^{2-})_2$  and  $(\text{V}^{5+})_2(\text{O}^{2-})_5$ . The  $\text{O}_{1s}$  spectra for EMD heat treated at  $350^\circ\text{C}$  for 4 h (Fig. 2, curve (a)) has two  $\text{O}_{1s}$  peaks at 530.0 and 531.4 eV due to Mn–O and Mn–OH, respectively [6], and  $\text{V}_2\text{O}_5$  obtained by heating  $\text{NH}_4\text{VO}_3$  at  $350^\circ\text{C}$  for 4 h gives a peak at 530.5 eV (Fig. 2, curve (d)). On the other hand, the products formed between EMD and  $\text{NH}_4\text{VO}_3$  at V/Mn atomic ratios of 0.11 and 1.0 at  $350^\circ\text{C}$  for 4 h yield an  $\text{O}_{1s}$  peak at 530.3–530.5 eV (Fig. 2, curves (b) and (c)), i.e., between those for EMD and  $\text{V}_2\text{O}_5$ , and the  $\text{O}_{1s}$  peak at the higher energy due to Mn–OH almost disappears. This suggests the formation of a new phase on the surface of the EMD particles. Using the peak areas of  $\text{Mn}_{2p}$ ,  $\text{V}_{2p}$  and  $\text{O}_{1s}$  spectra, the apparent surface compositions

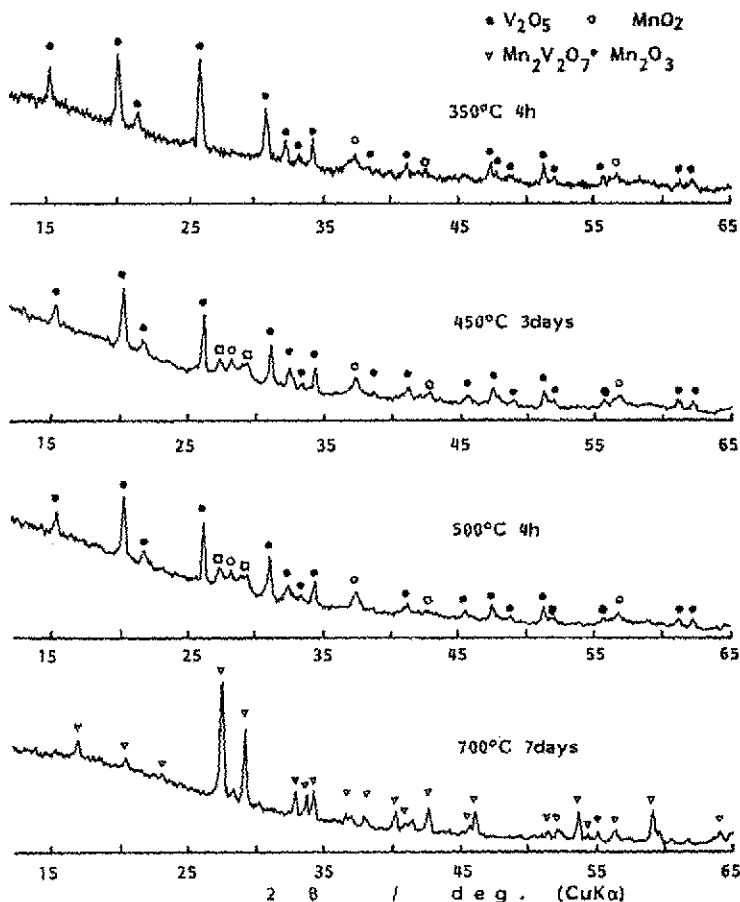


Fig. 1. XRD patterns for products from heat-treated mixtures of EMD and  $\text{NH}_4\text{VO}_3$  with a V/Mn atomic ratio of 1.0. Heat-treatment temperatures as shown.

of the products obtained from V/Mn atomic ratios of 0.10 and 1.0 were computed to be  $\text{Mn}_{1.00}\text{V}_{0.12}\text{O}_{2.22}$  and  $\text{Mn}_{1.00}\text{V}_{0.79}\text{O}_{4.21}$ , respectively. Electron micrographs of the heat treated products derived from a V/Mn atomic ratio of 1.0 at 350 °C and 700 °C are shown in Fig. 3(c) and (d), respectively, together with those for EMD (IBA No. 17) heat treated at 350 °C for 4 h (Fig. 3(a)), and  $\text{V}_2\text{O}_5$  obtained by heating  $\text{NH}_4\text{VO}_3$  at 350 °C for 4 h (Fig. 3(b)). It can be seen (Fig. 3(c)) that the product prepared at 350 °C consists of large EMD particles surrounded by many fine particles of  $\text{V}_2\text{O}_5$ .

In summary, XRD and ESCA spectrum measurements, together with SEM observations, suggest that the products formed between EMD and  $\text{NH}_4\text{VO}_3$  at 350–500 °C still consist mostly of  $\text{MnO}_2$  and  $\text{V}_2\text{O}_5$ , but a small amount of new phase, with  $\text{MnO}_2 \cdot x\text{V}_2\text{O}_5$  as the most likely composition, may be formed on the surface of the EMD particles.

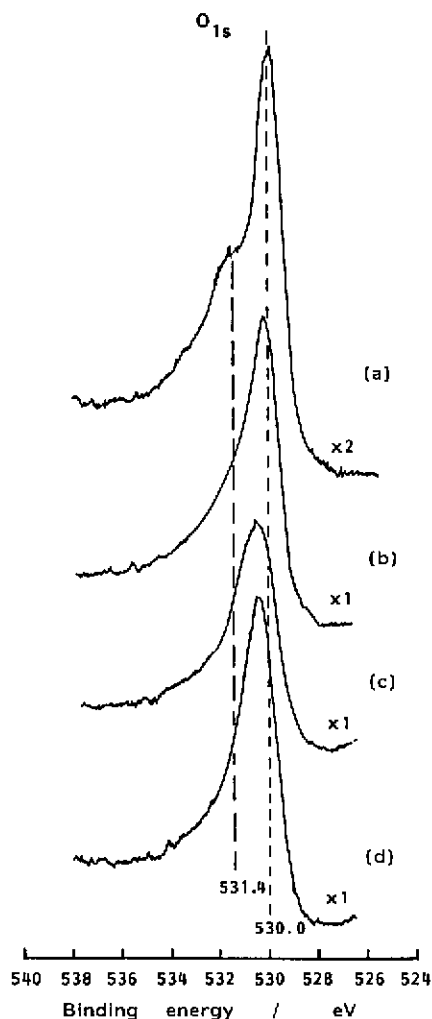


Fig. 2. ESCA  $O_{1s}$  spectra of EMD,  $V_2O_5$  and products of heat-treated EMD and  $NH_4VO_3$ . (a) EMD heat treated at 350 °C for 4 h in air; (b) composite for V/Mn atomic ratio of 0.11 at 350 °C for 4 h; (c) composite for V/Mn atomic ratio of 1.0 at 350 °C for 4 h; (d)  $V_2O_5$  from heating  $NH_4VO_3$  at 350 °C for 4 h in air.

#### *Charge/discharge cyclic characteristics of $MnO_2$ - $V_2O_5$ composites*

The charge/discharge characteristics of three types of  $MnO_2$  samples, viz., NMD (IC No. 7), CMD (IBA No. 22), and EMD (IBA No. 17), heat treated at 350 °C for 4 h were examined at a current density of 0.20 mA  $cm^{-2}$  and in 1 M  $LiClO_4$ -PC. NMD, CMD and EMD gave initial discharge capacities of about 40, 160, and 180 A h/kg-oxide, respectively, and potential plateaux at about 2.8 V versus  $Li/Li^+$ . For all samples, the capacity decreased to 50% of the initial value during charge/discharge cycles. A similar poor cycling behaviour of  $MnO_2$  has been reported previously [1-3].

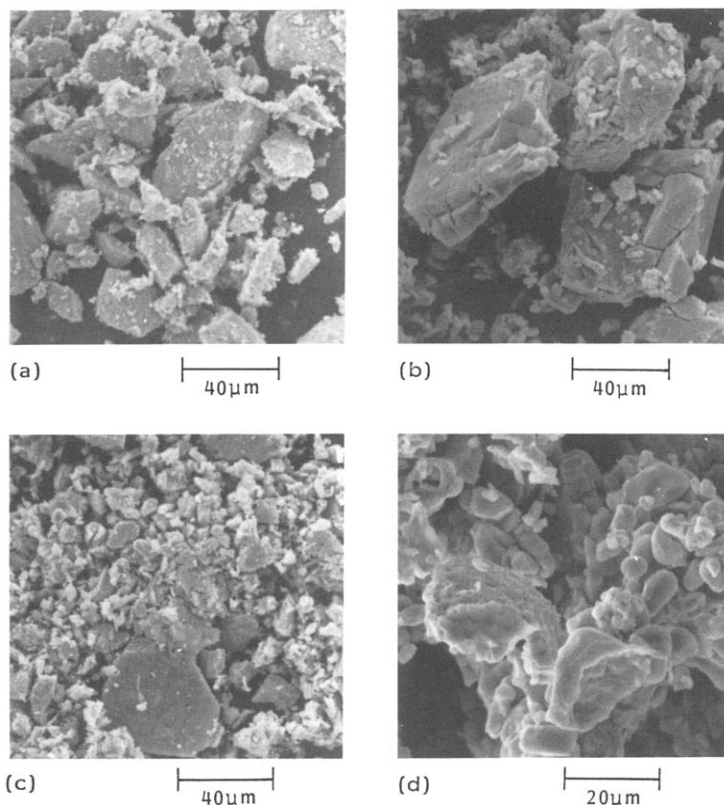


Fig. 3. SEM photographs of: (a) EMD (350 °C, 4 h); (b)  $V_2O_5$  from  $NH_4VO_3$  (350 °C, 4 h); (c) composite ( $V/Mn=1.0$ , 350 °C, 4 h); (d) composite ( $V/Mn=1.0$ , 700 °C, 7 days).

Figure 4 shows typical charge/discharge characteristics for oxide composites obtained by heating different  $MnO_2$  and  $NH_4VO_3$  mixtures with a  $V/Mn$  atomic ratio of 1.0 at 350 °C for 4 h. Clearly, the charge/discharge behaviour is strongly dependent upon the type of  $MnO_2$ . For composites obtained from EMD and CMD, the initial discharge curves consist of four main steps, including a potential plateau around 2.8 V versus  $Li/Li^+$  that is probably due to the discharge of  $MnO_2$  in the composite. The composite prepared from EMD exhibits the best cycling behaviour, and yields the highest capacity and energy density, viz., 220–330 A h/kg-oxide and 460–660 W h/kg-oxide, respectively.

Charge/discharge curves for composites obtained from an EMD and  $NH_4VO_3$  mixture at a  $V/Mn$  atomic ratio of 1.0 and at various heat-treatment temperatures are presented in Fig. 5. The capacities on the 1st and 5th cycles decrease as the temperature is raised. At temperatures above 450 °C, the potential plateau of the initial discharge at about 2.7 V, due to the discharge of  $MnO_2$ , is reduced considerably. This may result from the growth

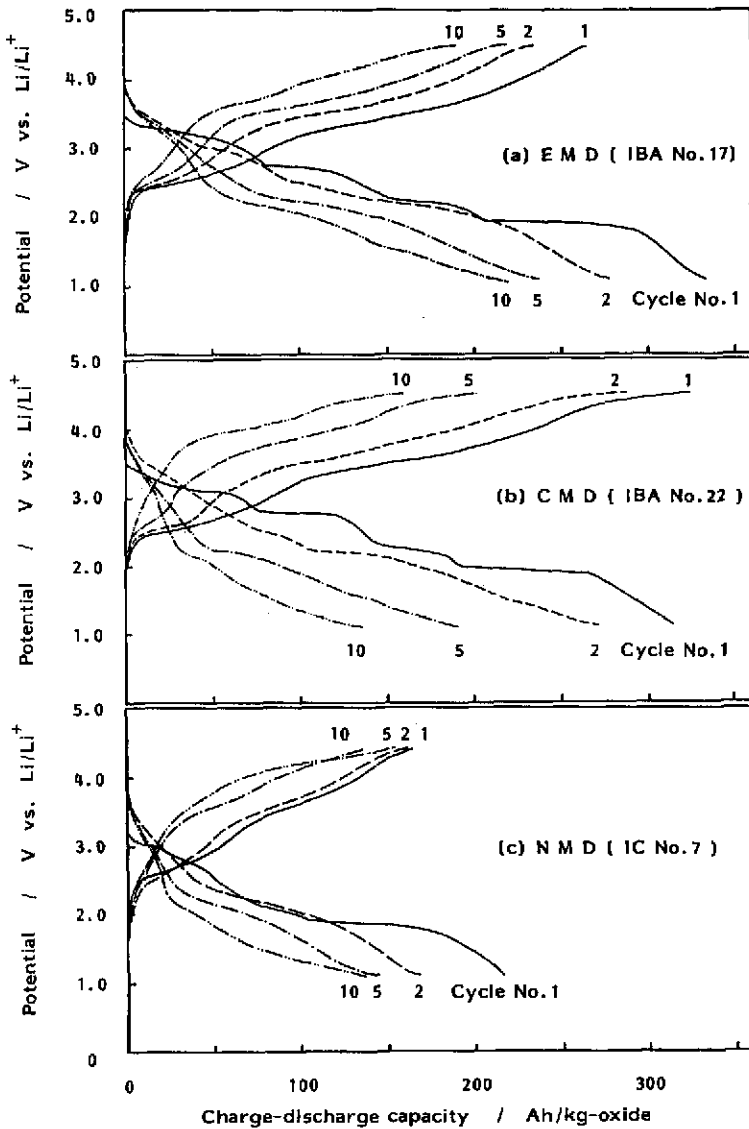


Fig. 4. Charge/discharge curves for composites from heating  $\text{NH}_4\text{VO}_3$  and different  $\text{MnO}_2$  types at a V/Mn ratio of 1.0 and at  $350^\circ\text{C}$  for 4 h. Current density =  $0.20\text{ mA cm}^{-2}$ ; cut-off potentials: 1.10 V (discharge) and 4.40 V (charge).

of a new surface layer formed on the EMD particles. The highest capacity was obtained at  $350^\circ\text{C}$ . At this temperature, the charge/discharge behaviour exhibited little dependence on the heat-treatment time over the range 4–72 h.

For composites obtained by heating EMD and  $\text{NH}_4\text{VO}_3$  mixtures at various V/Mn atomic ratios between 0.1 and 2.0 at  $350^\circ\text{C}$  for 4 h, the discharge capacities on the 1st and 5th cycles increased with increasing V/Mn atomic

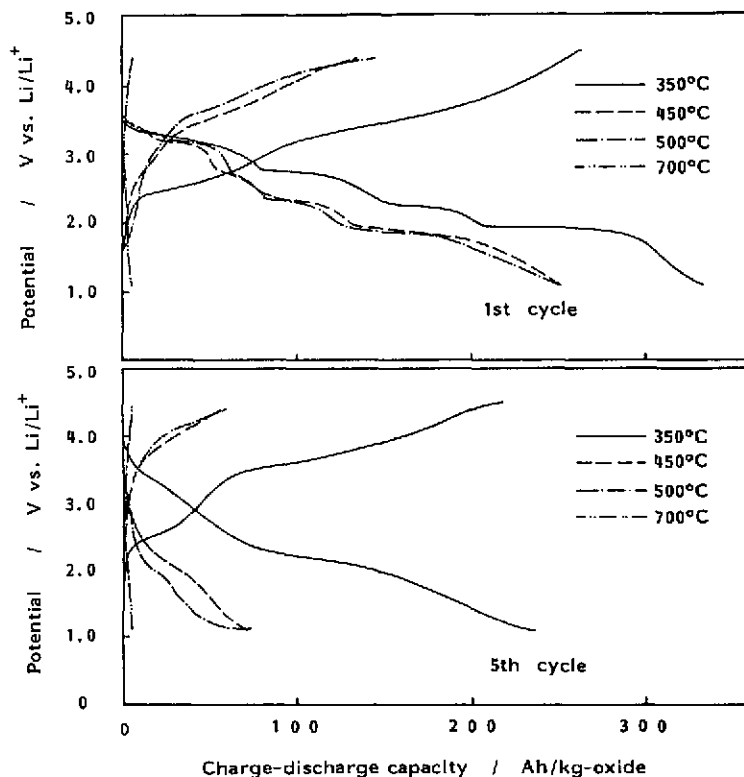


Fig. 5. Charge/discharge curves for composites from heating EMD and  $\text{NH}_4\text{VO}_3$  at a V/Mn atomic ratio of 1.0 and at various temperatures for 4 h. Current density =  $0.20 \text{ mA cm}^{-2}$ .

ratio. The highest capacities of 330–350 (1st cycle) and 230–270 A h/kg-oxide (5th cycle) were obtained for a V/Mn ratio of 1.0–2.0.

The charge/discharge curves of a composite (with V/Mn = 1.0 and heated at  $350^\circ\text{C}$  for 4 h) at several current densities are shown in Fig. 6. The potential plateau at 2.8 V versus  $\text{Li/Li}^+$  (which may be associated with the discharge of  $\text{MnO}_2$ ) is considerably reduced at current densities  $> 1.0 \text{ mA cm}^{-2}$ . The capacity decreases with increasing current density. After 10 cycles at a current density of  $1.0 \text{ mA cm}^{-2}$ , the discharge capacity is  $\sim 160 \text{ A h/kg-oxide}$ .

Finally charge/discharge tests were conducted on a composite (EMD and  $\text{NH}_4\text{VO}_3$ , V/Mn atomic ratio = 1.0,  $350^\circ\text{C}$ , 4 h) at a constant capacity of  $40 \text{ A h/kg-oxide}$  and at  $0.50 \text{ mA cm}^{-2}$ . The results were compared with those obtained from similar experiments on  $\gamma/\beta\text{-MnO}_2$  and a mixture of  $\gamma/\beta\text{-MnO}_2$  and  $\text{V}_2\text{O}_5$  at a V/Mn atomic ratio of 1.0, see Fig. 7. It was confirmed that the oxide composite gives by far the best cycling performance.

#### *Structural change of $\text{MnO}_2\text{-V}_2\text{O}_5$ composite during discharge*

X-ray diffraction patterns for a composite (V/Mn = 1.0,  $350^\circ\text{C}$ , 4 h) taken to various depths of discharge are given in Fig. 8. During the initial

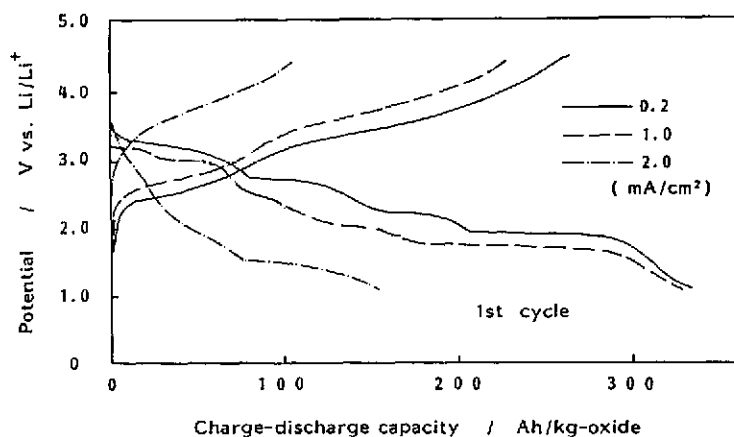


Fig. 6. Initial charge/discharge curves for a composite from EMD and  $\text{NH}_4\text{VO}_3$  ( $\text{V}/\text{Mn}=1.0$ ,  $350^\circ\text{C}$ , 4 h). Current densities as shown.

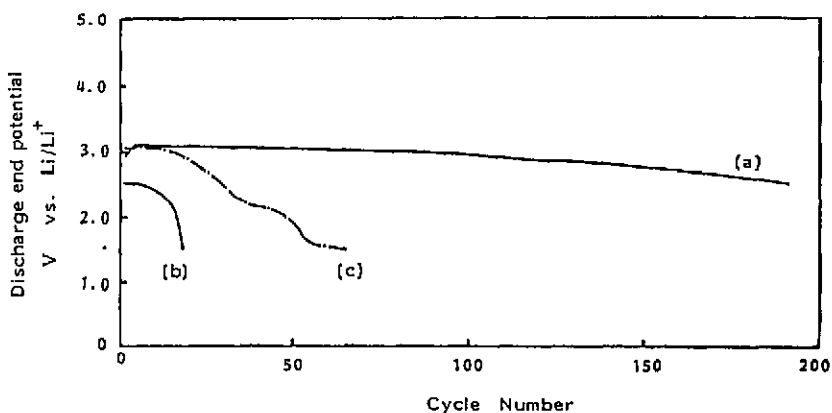


Fig. 7. Cycle performance at a constant capacity of 40 A h/kg-oxide and at  $0.50\text{ mA cm}^{-2}$ . (a) Composite from EMD and  $\text{NH}_4\text{VO}_3$  ( $\text{V}/\text{Mn}=1.0$ ,  $350^\circ\text{C}$ , 4 h); (b) EMD heat treated at  $350^\circ\text{C}$  for 4 h; (c) mixture of EMD heat treated at  $350^\circ\text{C}$  for 4 h and  $\text{V}_2\text{O}_5$  obtained from  $\text{NH}_4\text{VO}_3$  at  $350^\circ\text{C}$  ( $\text{V}/\text{Mn}=1.0$ ).

stage of discharge, a large change in the  $\text{V}_2\text{O}_5$  diffraction peaks is observed, i.e., the peaks lose intensity and broaden considerably, while the (001) peak (which gives the inter-layer distance) shifts to a lower  $2\theta$  position with increasing discharge. These observations are similar to those found with  $\text{V}_2\text{O}_5$  itself [7]. By contrast, the peak intensity of  $\text{MnO}_2$  decreases with discharge, and several new peaks, probably due to  $\text{LiMn}_2\text{O}_5$  [8], appear on discharge to 228 A h/kg-oxide, which corresponds to  $1.0 e^-/(\text{Mn} + \text{V})$ . These results indicate that, during discharge,  $\text{Li}^+$  ions are first inserted in the layered lattice of  $\text{V}_2\text{O}_5$  surrounding the  $\text{MnO}_2$  particles. This gives rise to an expansion along the  $c$ -axis of  $\text{V}_2\text{O}_5$ , i.e., from 4.371 to 4.572 Å. An increase in the unit-cell volume by  $\sim 3.0\%$  is caused by discharge to 71



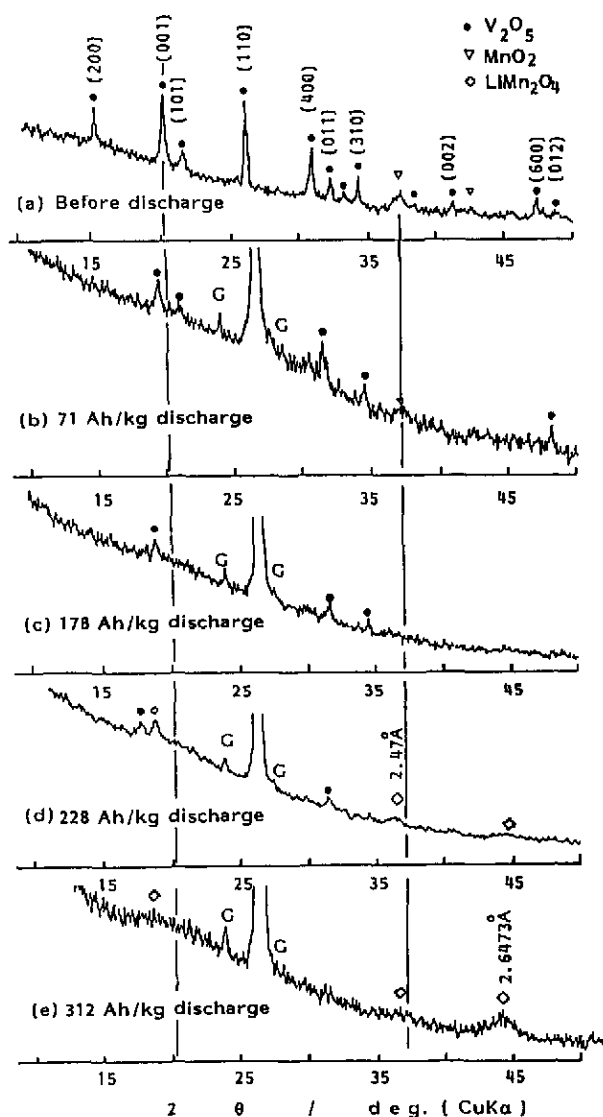


Fig. 8. XRD patterns of an  $\text{MnO}_2\text{-V}_2\text{O}_5$  composite discharged to various capacities. Starting active material: composite from EMD and  $\text{NH}_4\text{VO}_3$  mixture,  $\text{V/Mn} = 1.0$ ,  $350^\circ\text{C}$ , 4 h. G = graphitic.

A h/kg-oxide, which corresponds to  $0.3 e^-/(\text{Mn} + \text{V})$ . On further discharge to 100–200 A h/kg-oxide,  $\text{Li}^+$  ions are inserted in the crystal lattice of  $\text{MnO}_2$  through the surface layer and result in the formation of  $\text{LiMn}_2\text{O}_4$ . This is in agreement with the change in the discharge potential of the composite, as witnessed in Fig. 4. Finally, the crystal structure of the composite discharged to various capacities (70–230 A h/kg-oxide) does not recover to the initial state after charging.

Charge/discharge capacities of the composites obtained from EMD and  $\text{NH}_4\text{VO}_3$  mixtures decrease with increasing heat-treatment temperature (Fig. 5), and the composite (V/Mn = 1.0, 350 °C, 4 h) shows considerably better cycling characteristics than a mixture of EMD and  $\text{V}_2\text{O}_5$  (Fig. 7). This behaviour is probably caused by the formation of a surface layer on the  $\text{MnO}_2$  particles. As shown from XRD and ESCA measurements (Figs. 1 and 2), the surface layer increases in quantity and becomes more crystalline as the heat-treatment temperature is raised above 400 °C. At the same time,  $\gamma/\beta\text{-MnO}_2$  is converted to the  $\beta$  polymorph that has smaller channels in the crystal structure [9]. On the other hand, at a temperature of  $\sim 350$  °C, the surface layer formed on the  $\text{MnO}_2$  may be the most suitable for the insertion and removal of  $\text{Li}^+$  ions into and from the bulk structure of  $\text{MnO}_2$ ; moreover, the crystal form of  $\gamma/\beta\text{-MnO}_2$  is maintained. These may be responsible for the excellent charge/discharge characteristics exhibited by the composite (Fig. 7).

### Acknowledgements

The authors thank Mrs Nobuko Kumagai for helpful assistance with the experimental work and also Mr Go Kawamura (Shinkobe Denki Co. in Japan) for helpful discussion.

### References

- 1 F. W. Dampier, *J. Electrochem. Soc.*, **121** (1974) 656.
- 2 G. Pistoia, *J. Electrochem. Soc.*, **129** (1982) 1861.
- 3 T. Nohma, T. Saito and N. Furukawa, *J. Power Sources*, **26** (1989) 389.
- 4 N. Kumagai and K. Tanno, *Denki Kagaku*, **50** (1982) 704.
- 5 *ASTM card 24-735*.
- 6 K. Hashimoto and K. Asami, *Boshoku Gijutzu*, **26** (1977) 375.
- 7 N. Kumagai and K. Tanno, *Denki Kagaku*, **48** (1980) 432.
- 8 *ASTM card 18-736*.
- 9 M. Jansen and R. Hoppe, *Z. Anorg. Allg. Chem.*, **397** (1973) 279.